

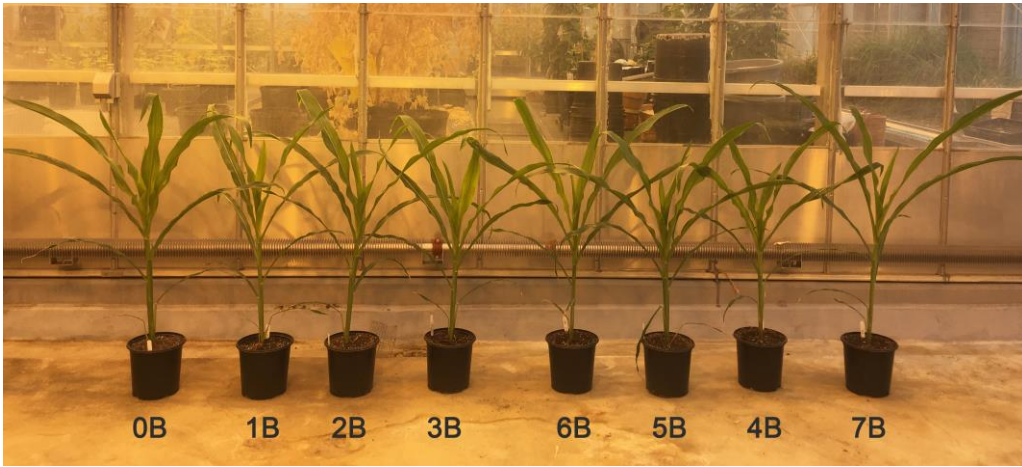
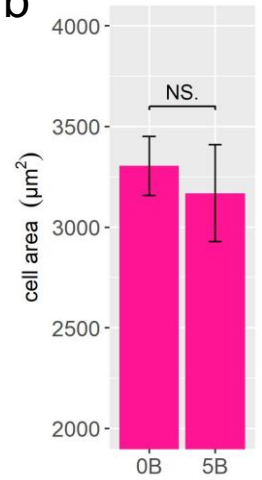
a**b**

Figure S1. The phenotype of experimental genotypes (1B-7B) and the control (0B) and the cell size comparison. **(a)** The phenotype of the B dosage series grown in the greenhouse. **(b)** Cell area of 5B plants (n=2) in comparison to the control (0B, n=4). NS., Student's t-test of means not statistically significant (P -value > 0.05).

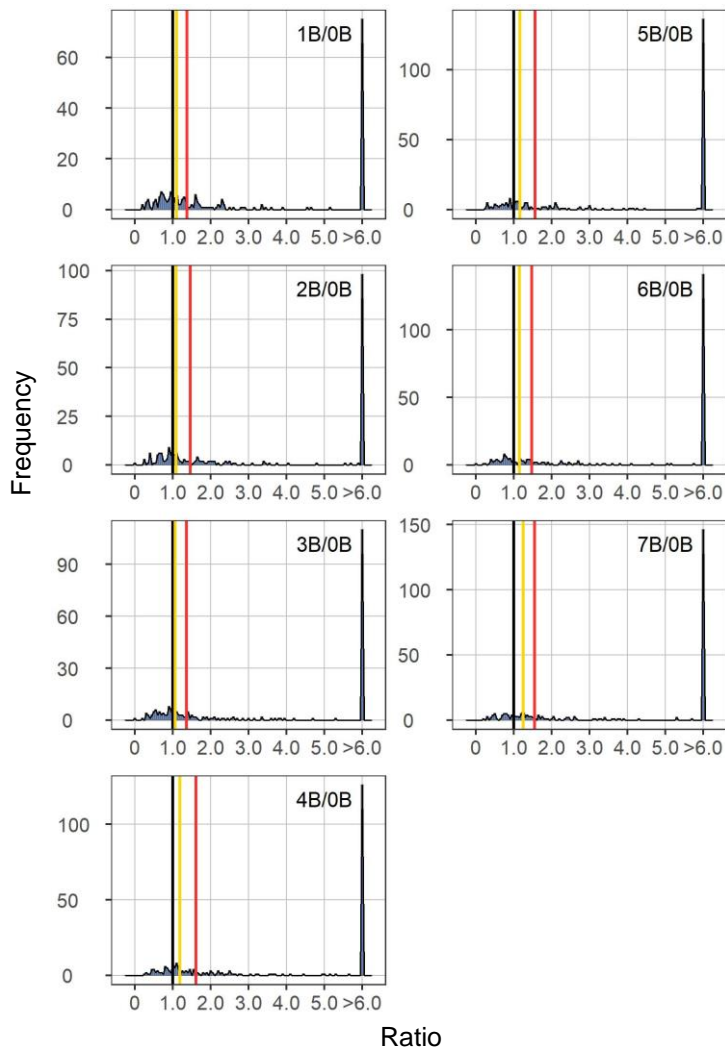


Figure S2. Ratio distributions of expression of B-located genes in each experimental genotype compared with the control with outliers (ratio > 6 or < 1/6) included. Plots were generated as described in Figure 1.

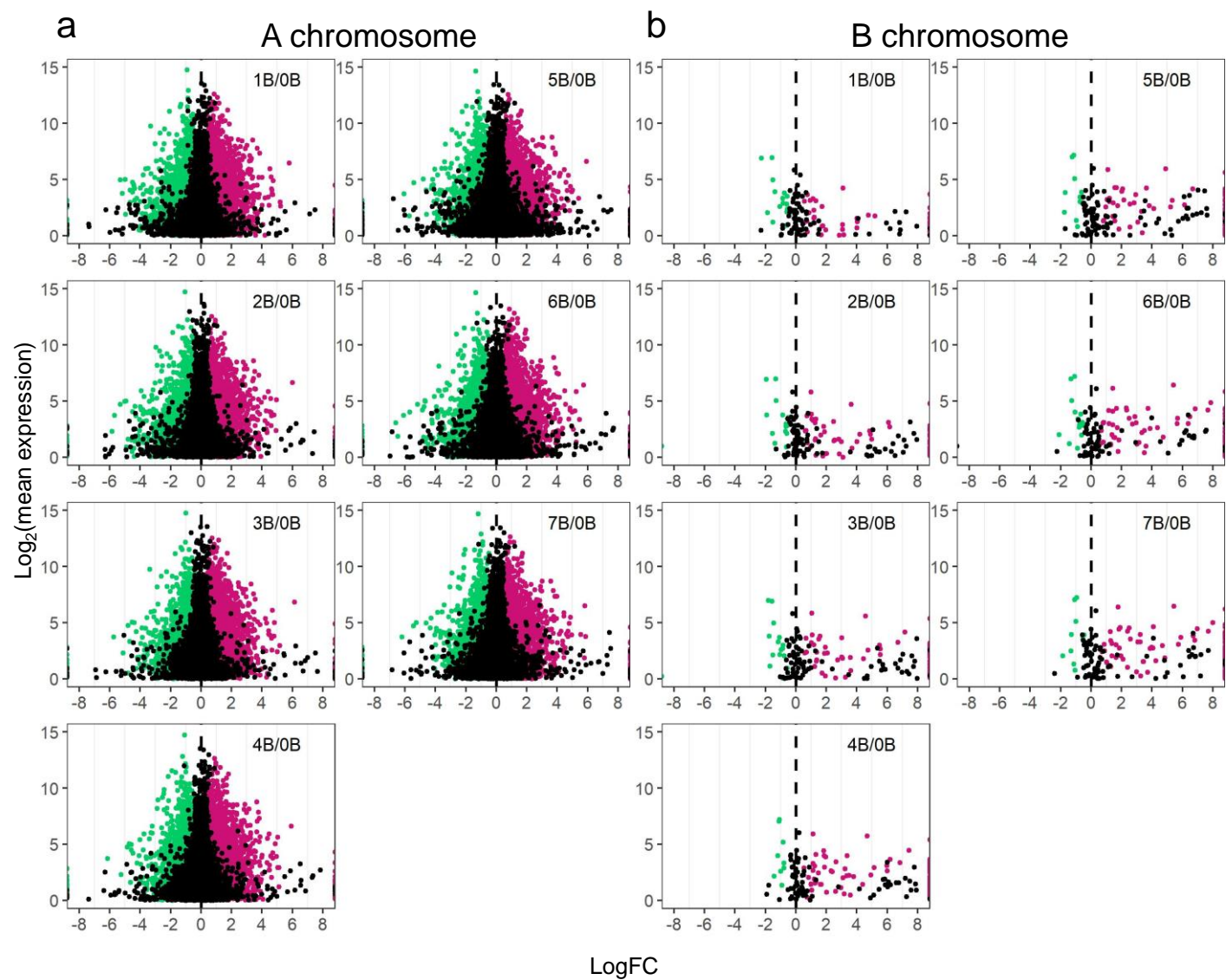


Figure S3. Scatter plots of DGE in each experimental genotype compared with the control. **(a)** Scatter plots of A-located genes. **(b)** Scatter plots of B-located genes. Plots were generated as described in Figure 5.

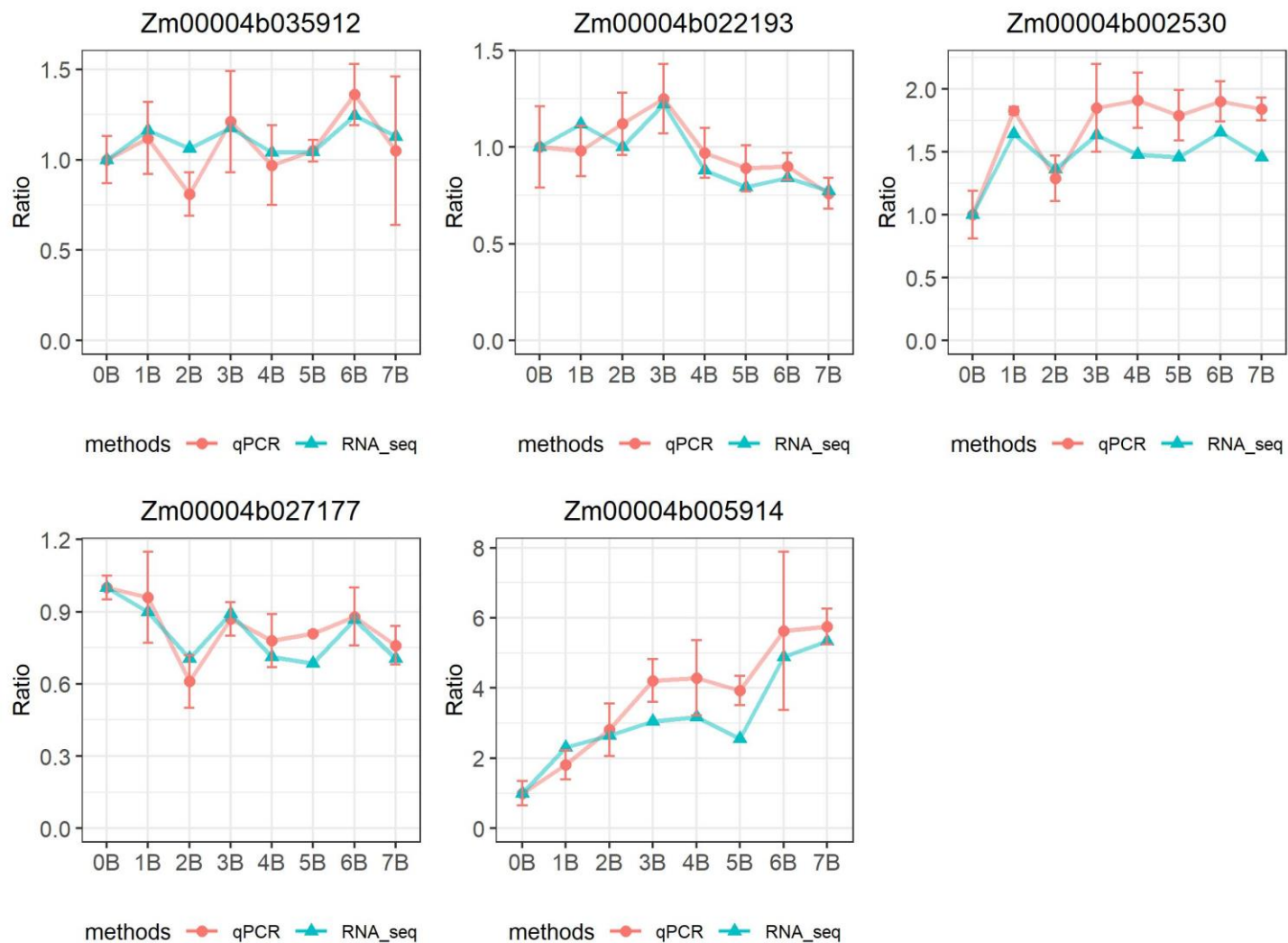


Figure S4. Gene ratios measured by qPCR compared with those computed by RNA-seq. Genes with different expression patterns were selected. Error bar represents SD. Except for 5B which only have 2 biological replicates, 3 biological replicates were used for other genotypes.

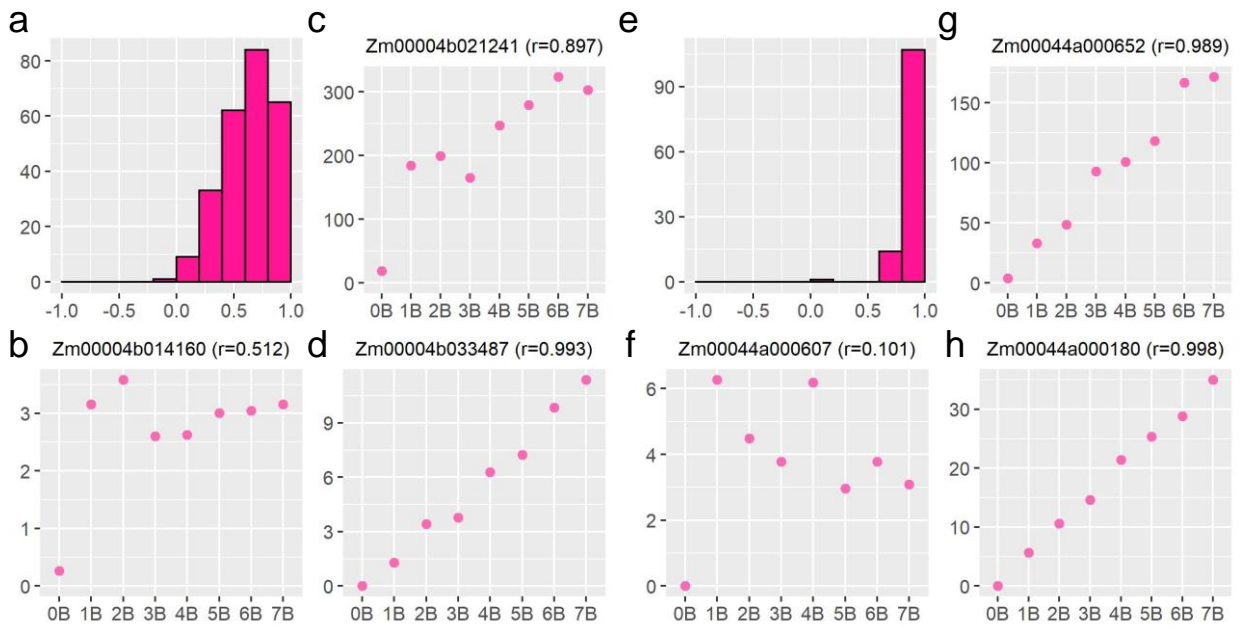


Figure S5. Gene expression level of outliers and PCC with B copy number (ratio > 6 or $< 1/6$). Analyses were performed as described in Figure 3. **(a and e)** Histogram of PCC between the expression level of A-located outliers **(a)** or B-located outliers **(e)** and the B copy number. **(b-d)** Example outliers from genes in **(a)** with distinct expression patterns and different values of PCC. **(f-h)** Example outliers from genes in **(e)** with distinct expression patterns and different values of PCC. The label of each panel represents the gene ID and the PCC value (r) showing the B-dosage sensitivity.

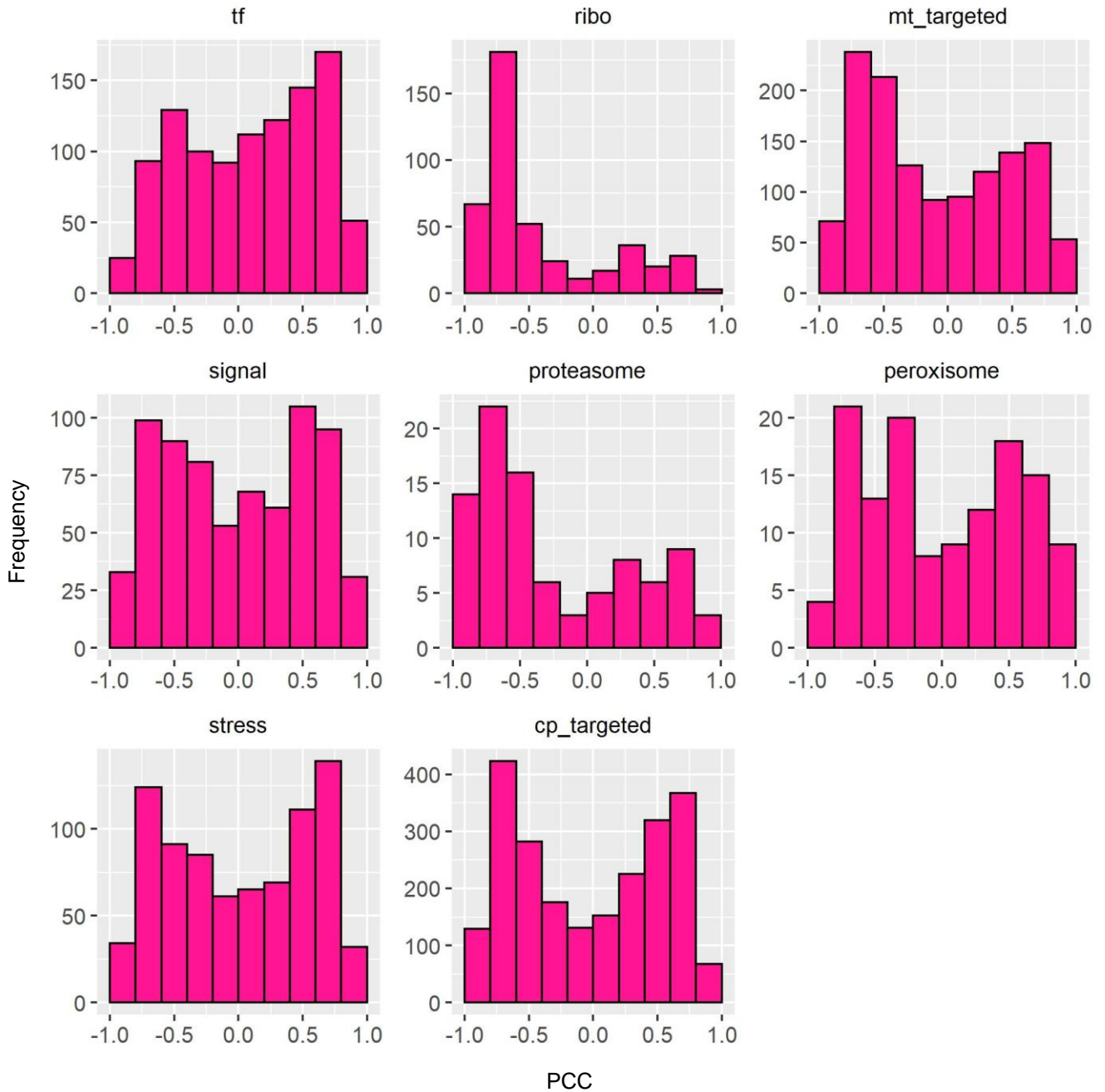


Figure S6. Histogram of PCC between the expression level of A-located genes from each functional class and B copy number. Plots were generated as described in Figure 3. cp, chloroplast; mt, mitochondrial.

Transcription factors

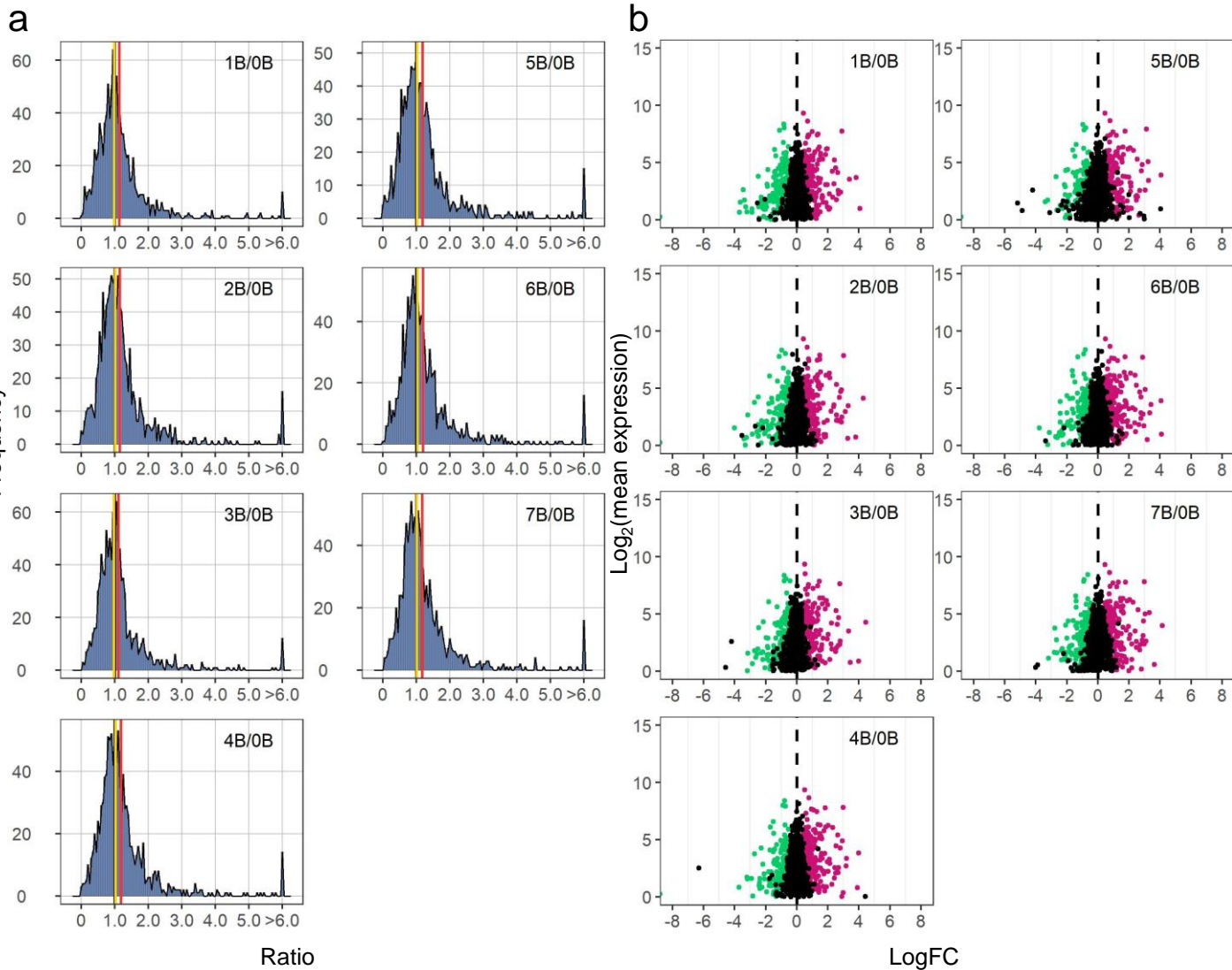


Figure S7. Ratio distributions and scatter plots of DGE for the functional class of TFs. Distributions **(a)** were generated as described in Figure 1, while scatter plots **(b)** were generated as described in Figure 5.

Signal transduction

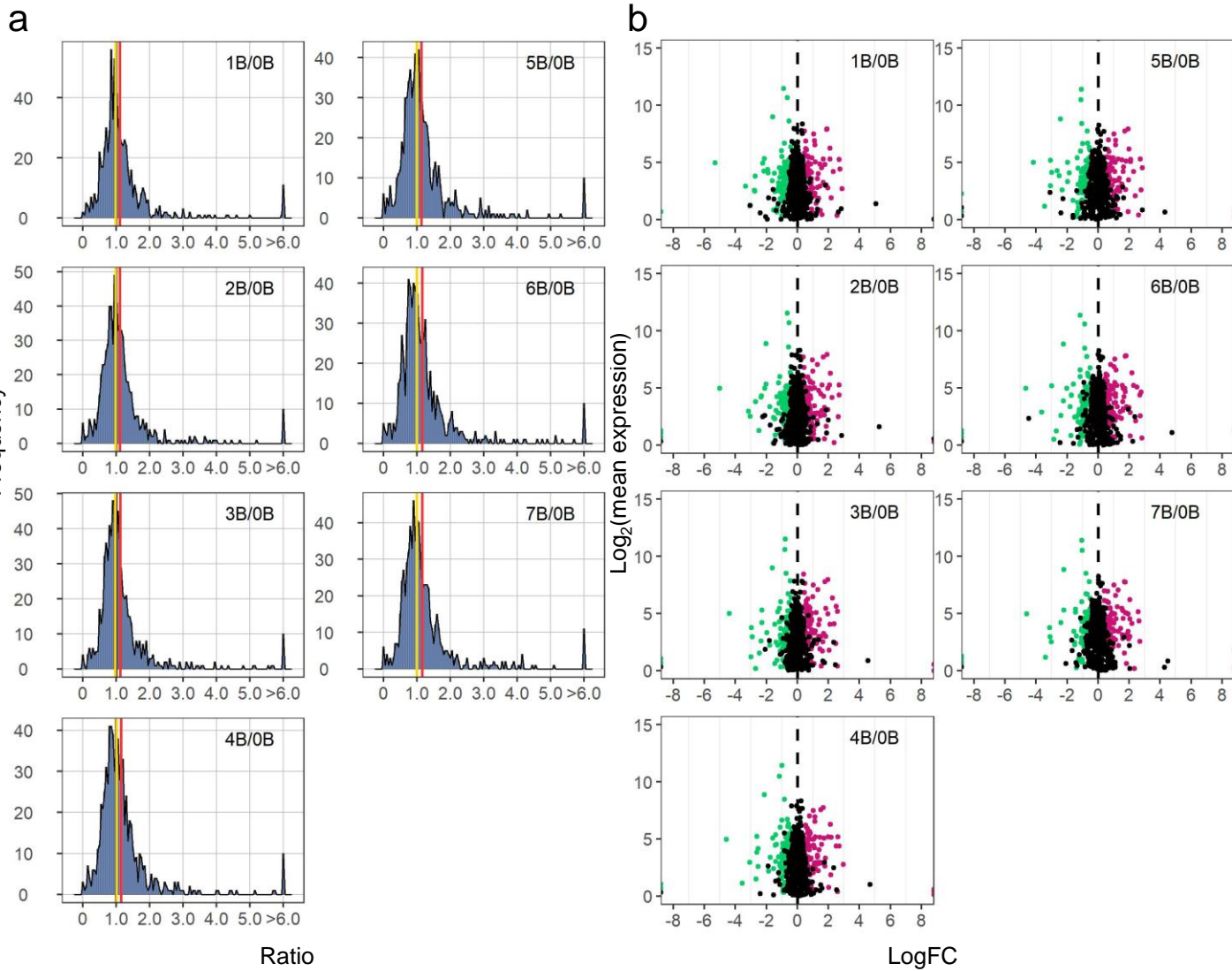


Figure S8. Ratio distributions and scatter plots of DGE for the functional class of signal transduction. Distributions (a) were generated as described in Figure 1, while scatter plots (b) were generated as described in Figure 5.

Proteasome

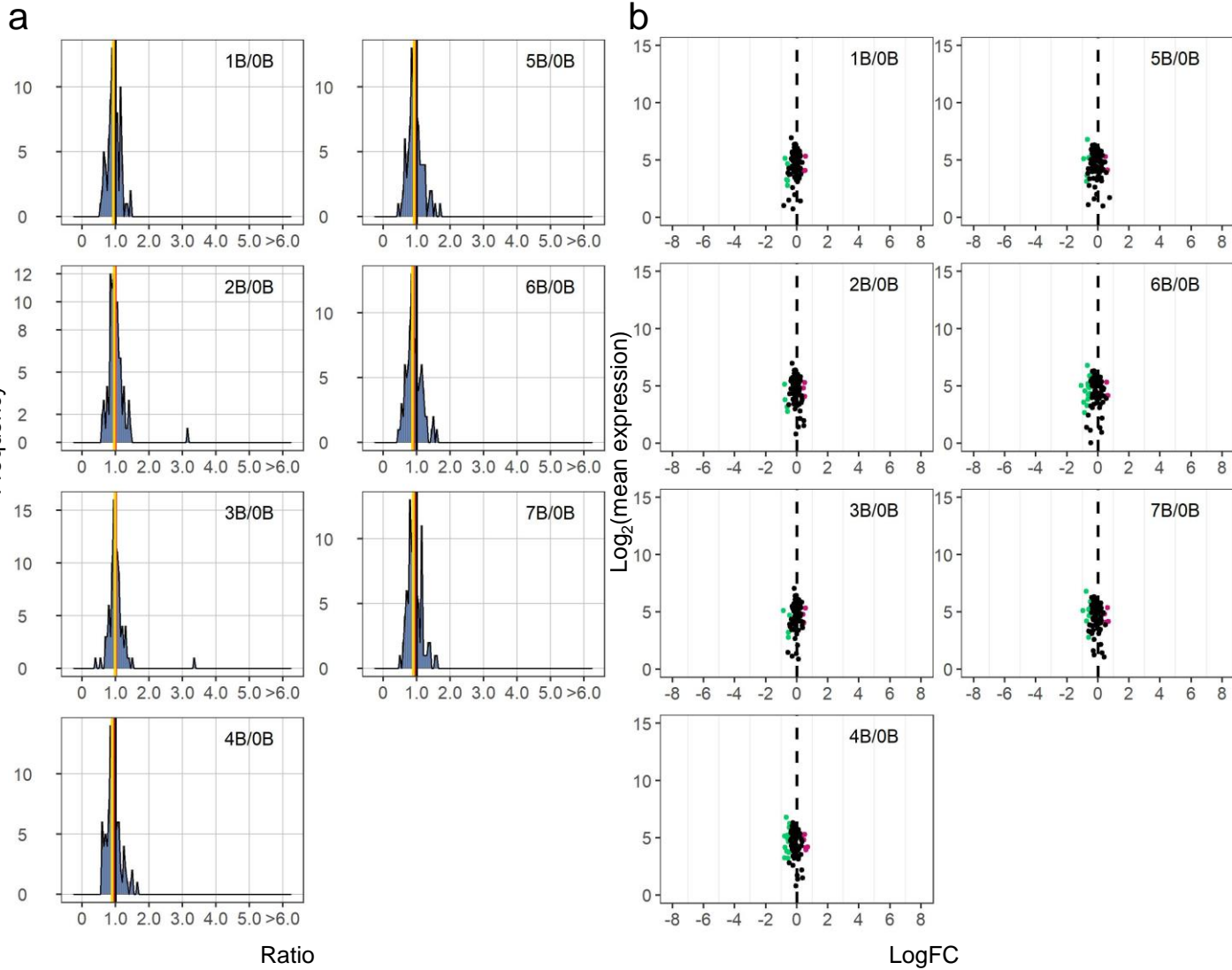


Figure S9. Ratio distributions and scatter plots of DGE for the functional class of structural proteins of the proteasome. Distributions (a) were generated as described in Figure 1, while scatter plots (b) were generated as described in Figure 5.

Stress related genes

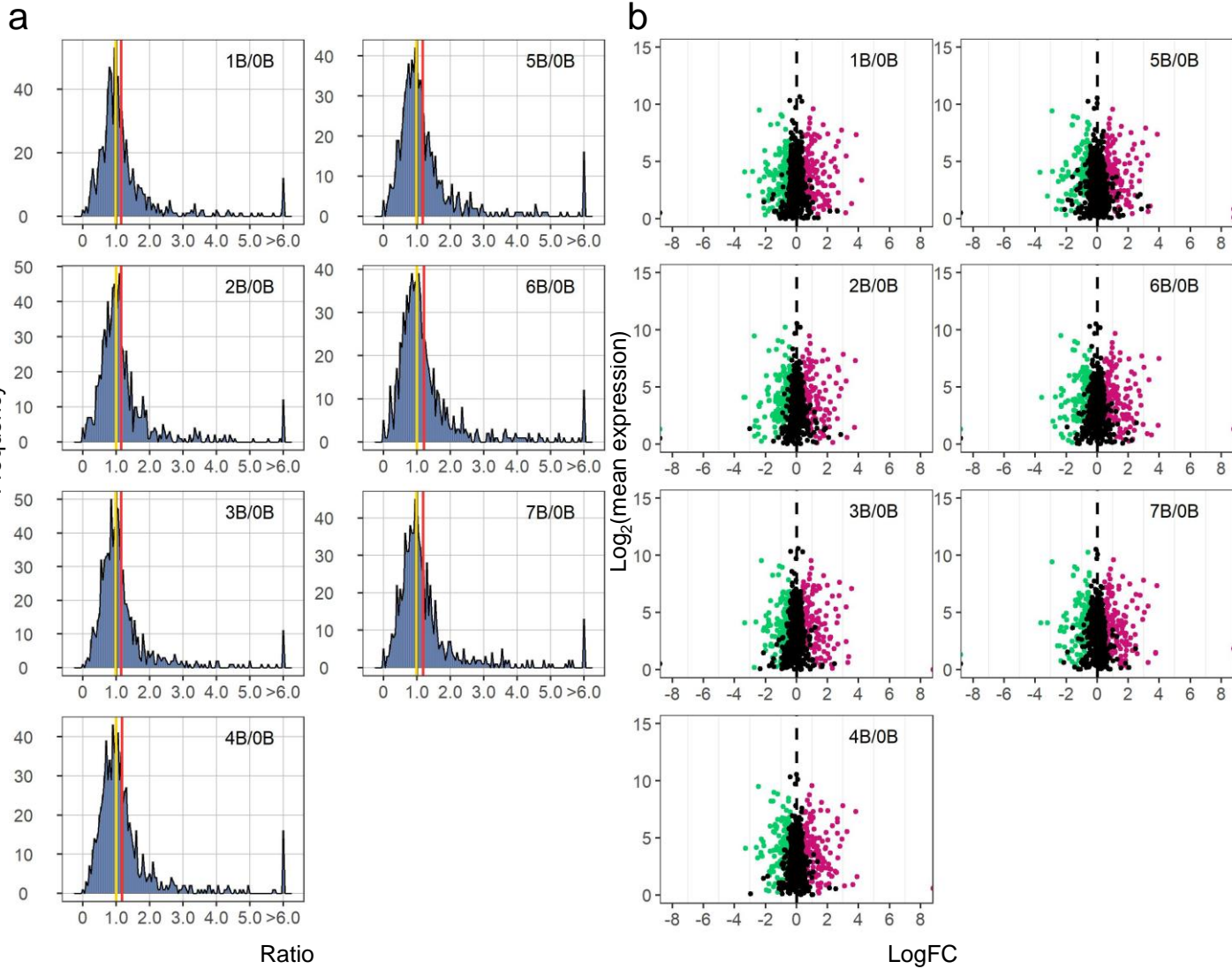


Figure S10. Ratio distributions and scatter plots of DGE for the functional class of stress-related genes. Distributions **(a)** were generated as described in Figure 1, while scatter plots **(b)** were generated as described in Figure 5.

Nuclear chloroplast genes

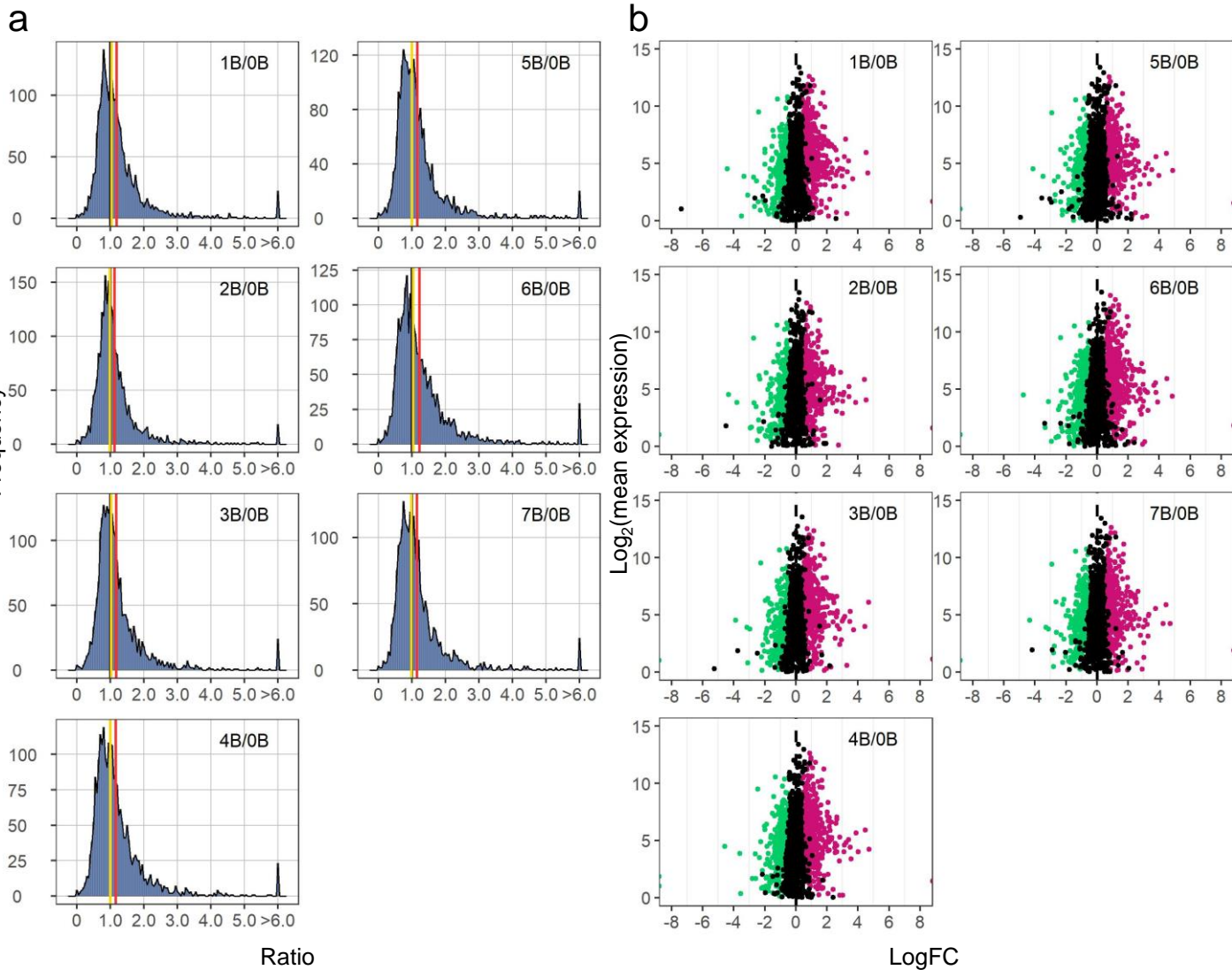


Figure S11. Ratio distributions and scatter plots of DGE for the functional class of nuclear chloroplast genes. Distributions **(a)** were generated as described in Figure 1, while scatter plots **(b)** were generated as described in Figure 5.

Nuclear mitochondrial genes

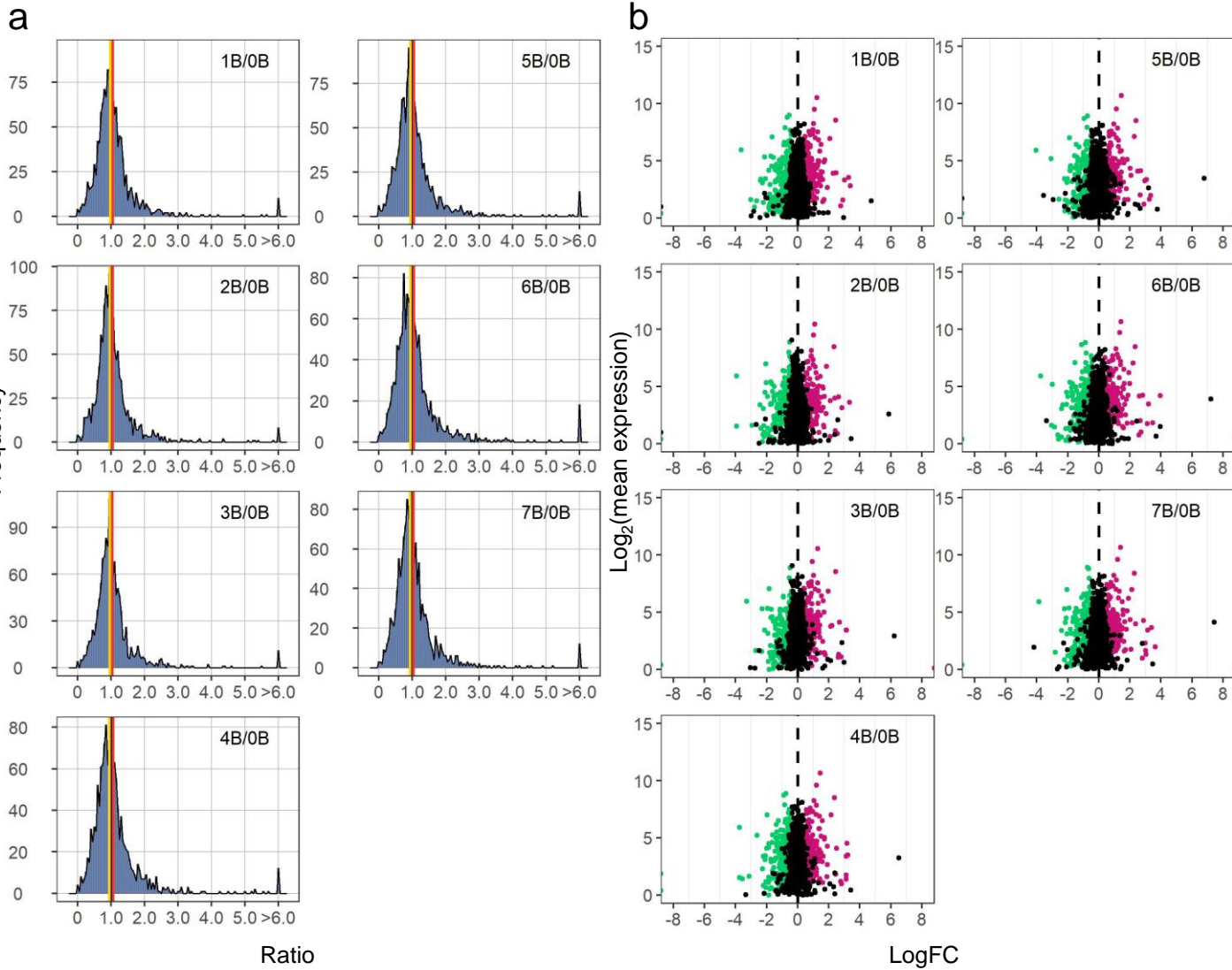


Figure S12. Ratio distributions and scatter plots of DGE for the functional class of nuclear mitochondrial genes. Distributions (a) were generated as described in Figure 1, while scatter plots (b) were generated as described in Figure 5.

Peroxisomal-targeted genes

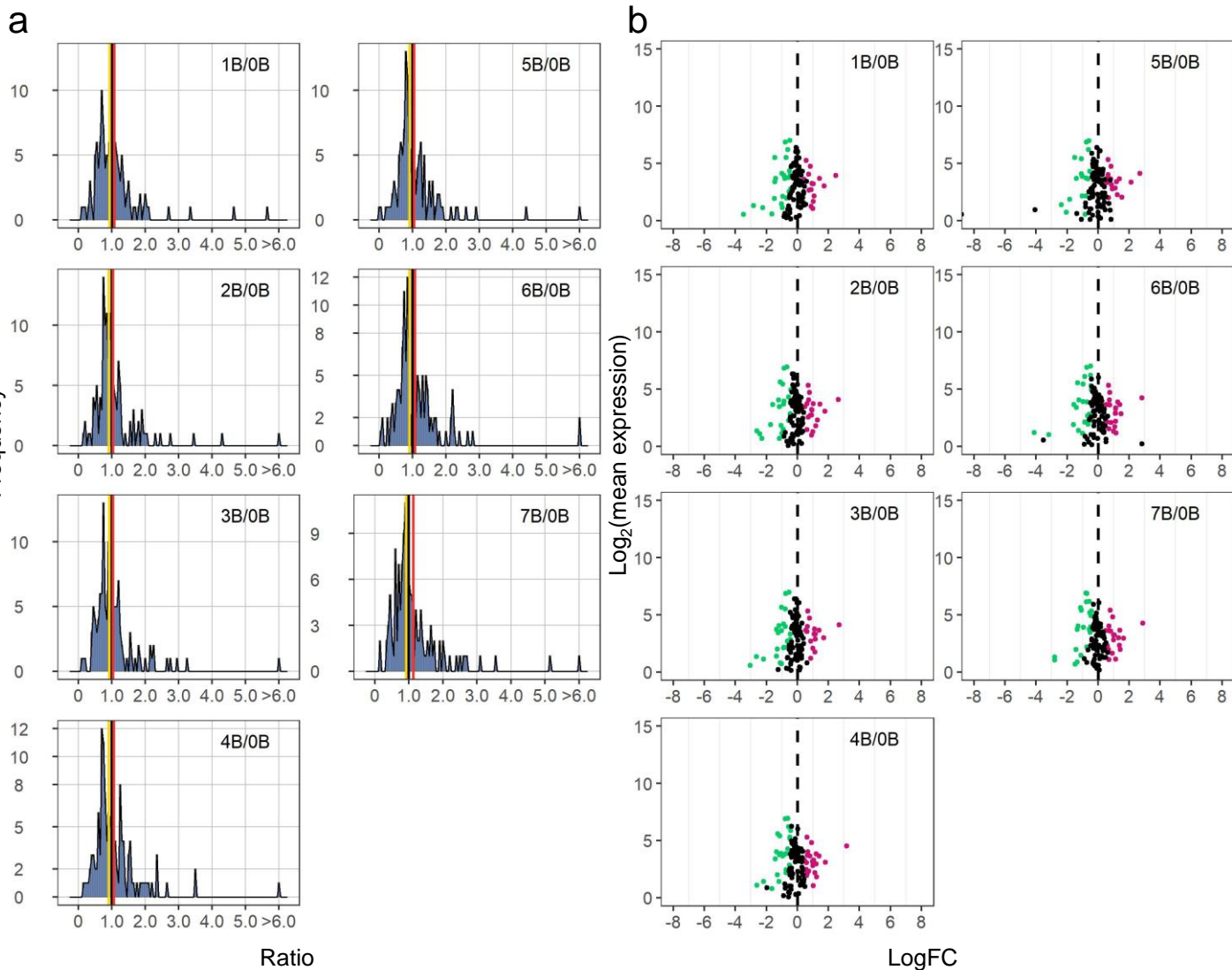


Figure S13. Ratio distributions and scatter plots of DGE for the functional class of peroxisomal-targeted genes. Distributions (a) were generated as described in Figure 1, while scatter plots (b) were generated as described in Figure 5.

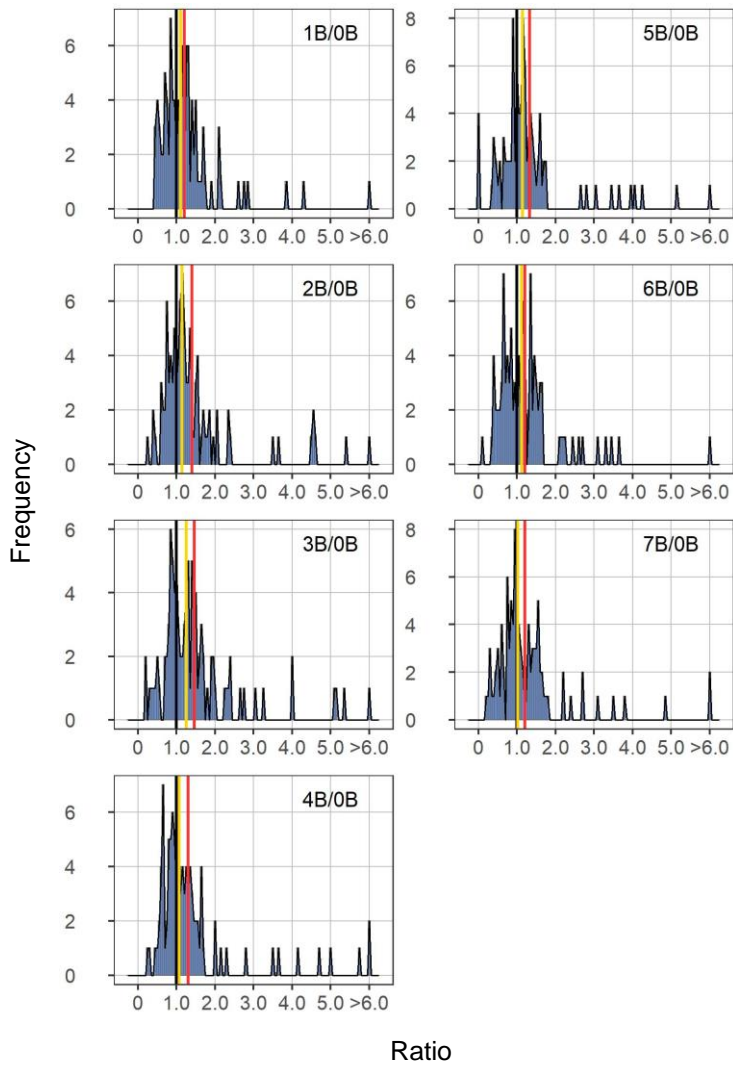


Figure S14. Ratio distributions of A-located miRNAs and B copy numbers. Ratio distributions were generated as described in Figure 1.

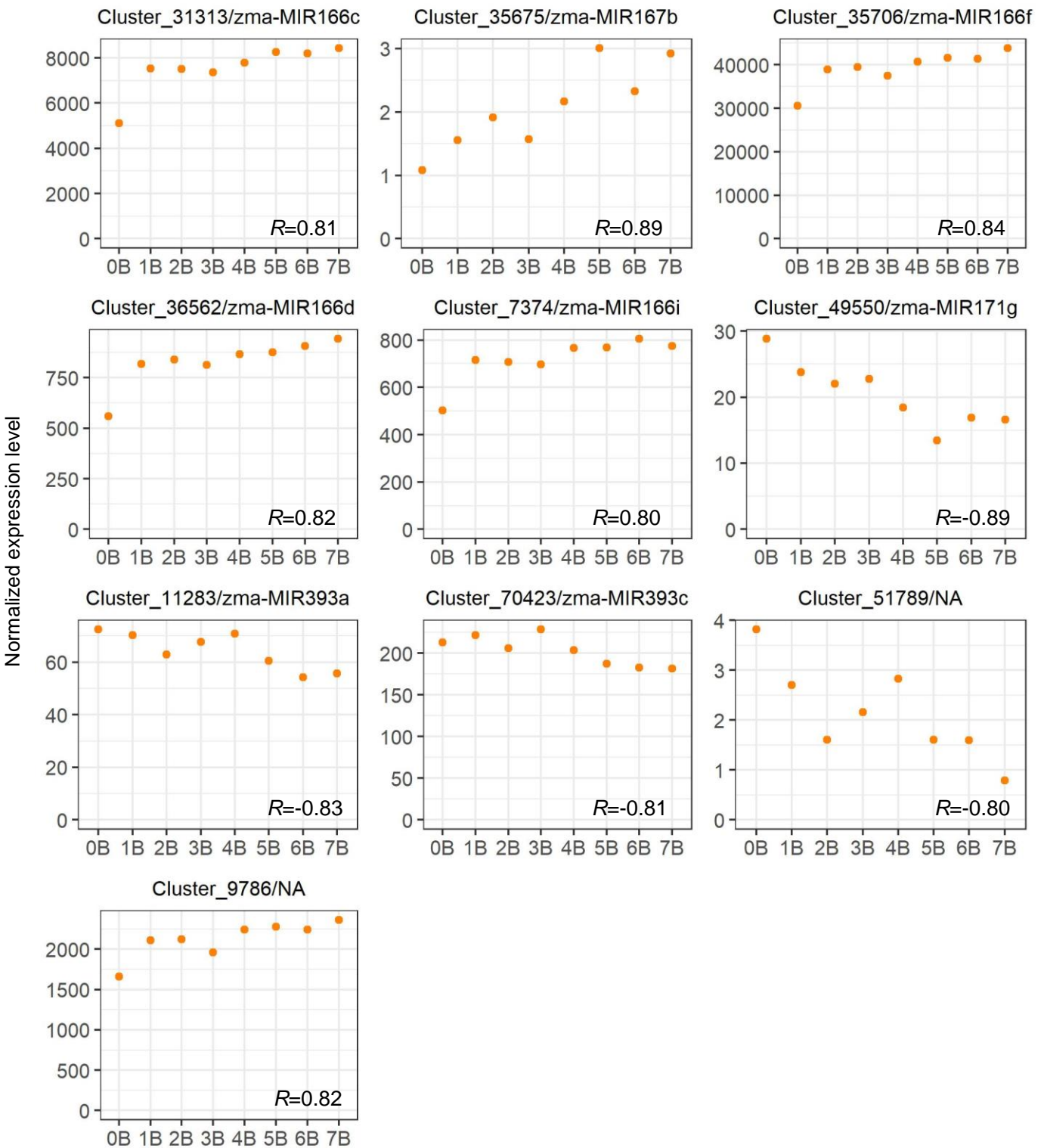


Figure S15. Expression levels of miRNAs that are sensitive to B dosage. Y-axis refers to the normalized expression level for each miRNA. X-axis notes the genotype. NA, miRNAs that are not annotated in miRbase version 22. *R*, PCC between expression levels of miRNAs and B copy number.

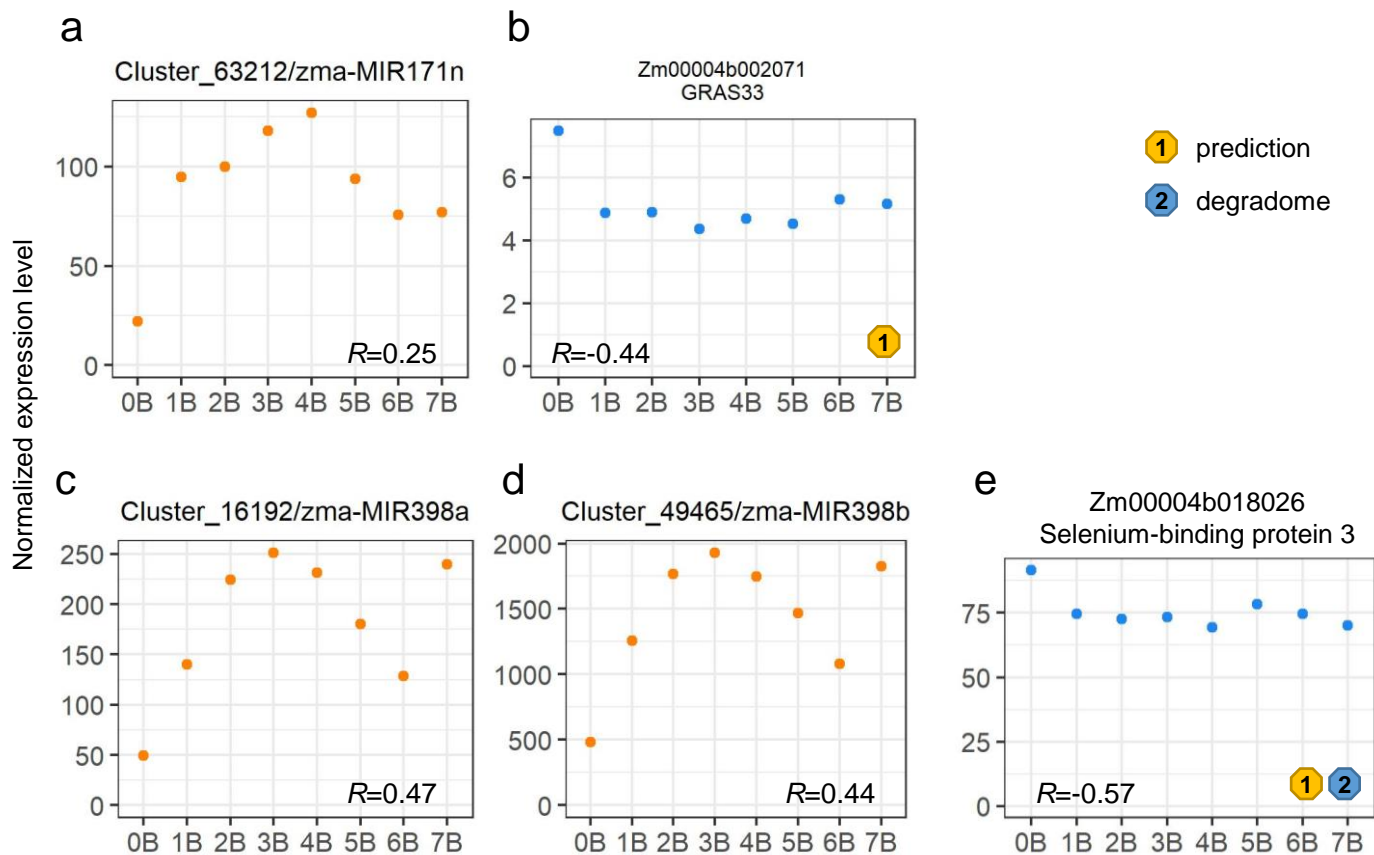


Figure S16. Expression levels of miRNAs and their targets in the B dosage series. Targets are predicted by psRNATarget (1) or gathered from results of degradome sequencing (2) as described in Material and Methods. Pearson correlation indicates a significant linear correlation between expression levels of each miRNA and its corresponding target (P -value < 0.05). **(b)** is predicted to be the target of **(a)**, while **(e)** is the target for both **(c)** and **(d)**. R , PCC between expression levels of DEM or target and B copy number.

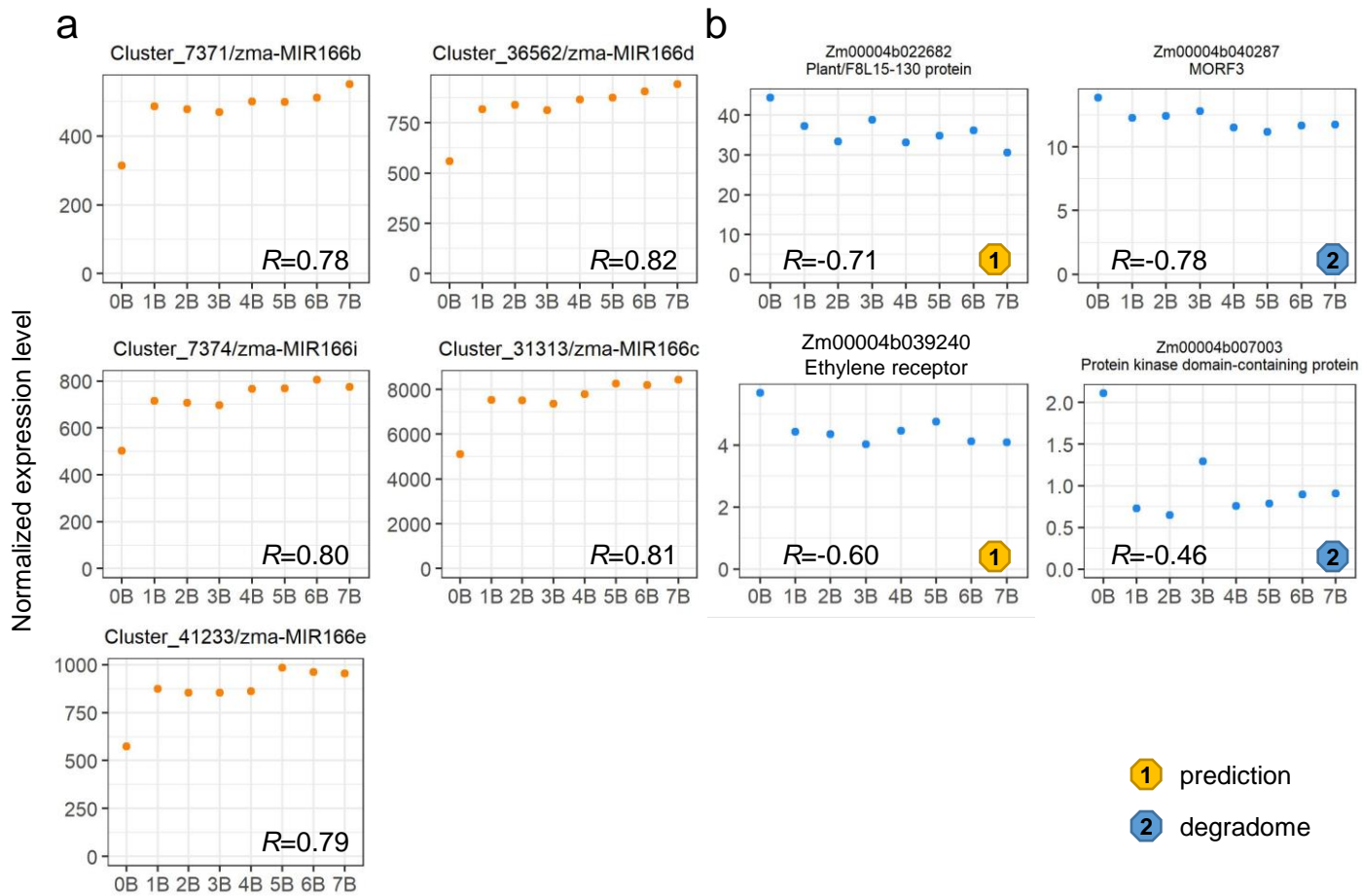


Figure S17. Expression levels of the family members of zma-MIR166 and their targets in the B dosage series, indicating different members of the same family have the same targets. Plots were generated as in Figure S15. Genes in **(b)** are the targets of miRNAs in **(a)**. R , PCC between expression levels of DEM or target and B copy number.

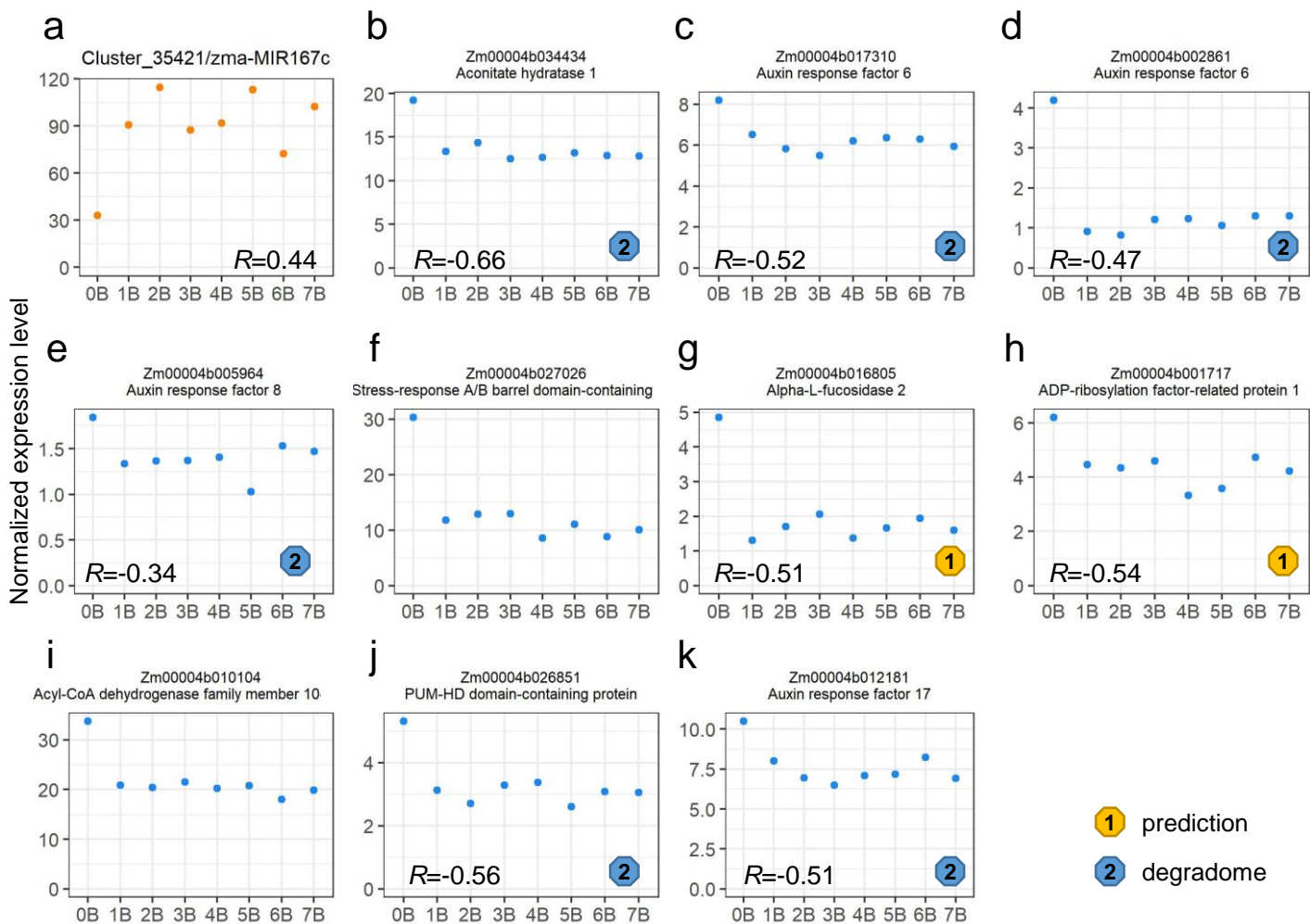


Figure S18. Expression levels of zma-MIR167c and its targets in the B dosage series. Plots were generated as in Figure S15. **(b-k)** are targets of **(a)**. *R*, PCC between expression levels of DEM or target and B copy number.

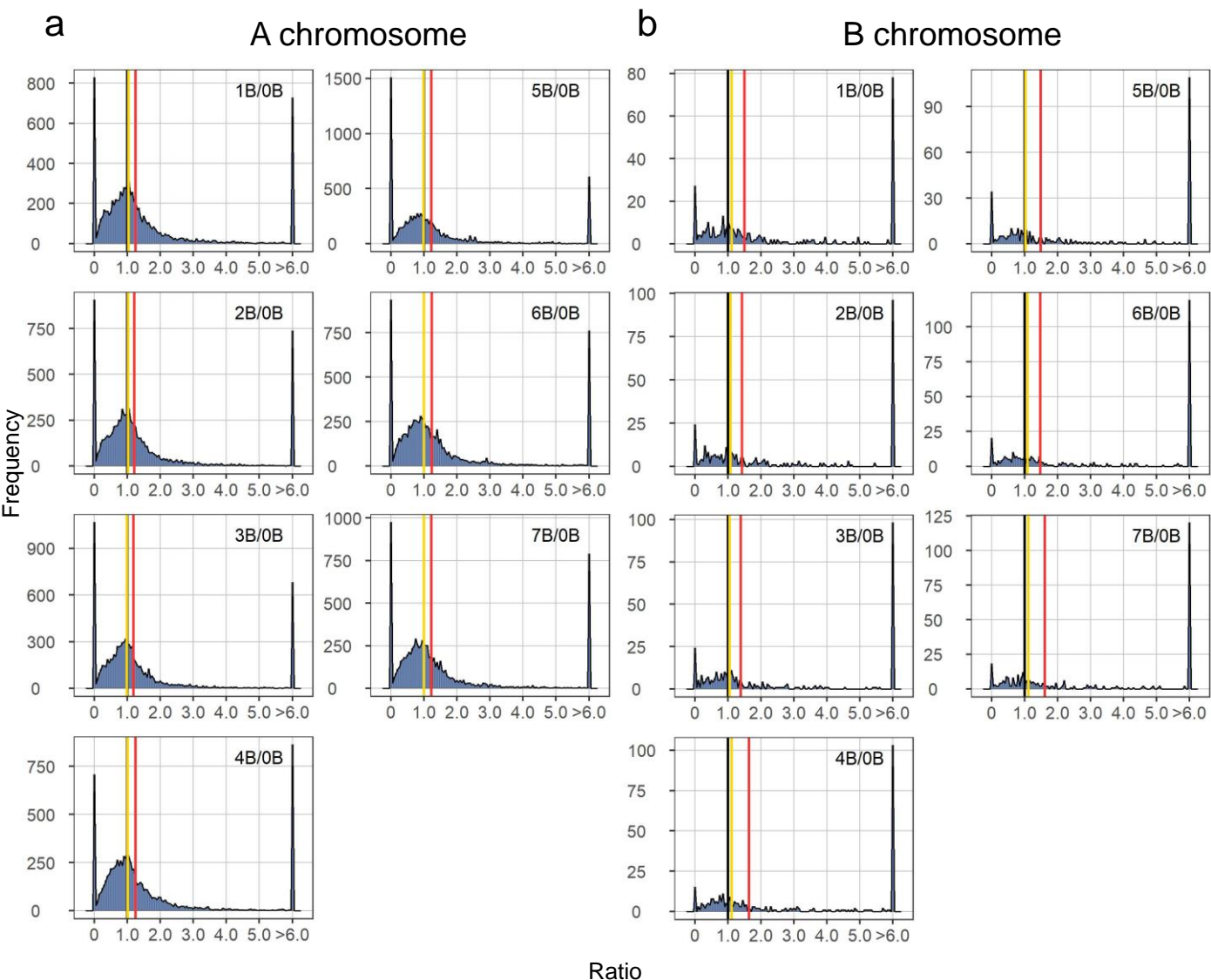


Figure S19. Ratio distributions and scatter plots of differential expression for all TEs. Distributions of A-located (a) and B-located (b) TEs were generated as described in Figure 1, while scatter plots of A-located (c) and B-located (d) TEs were generated as described in Figure 5.

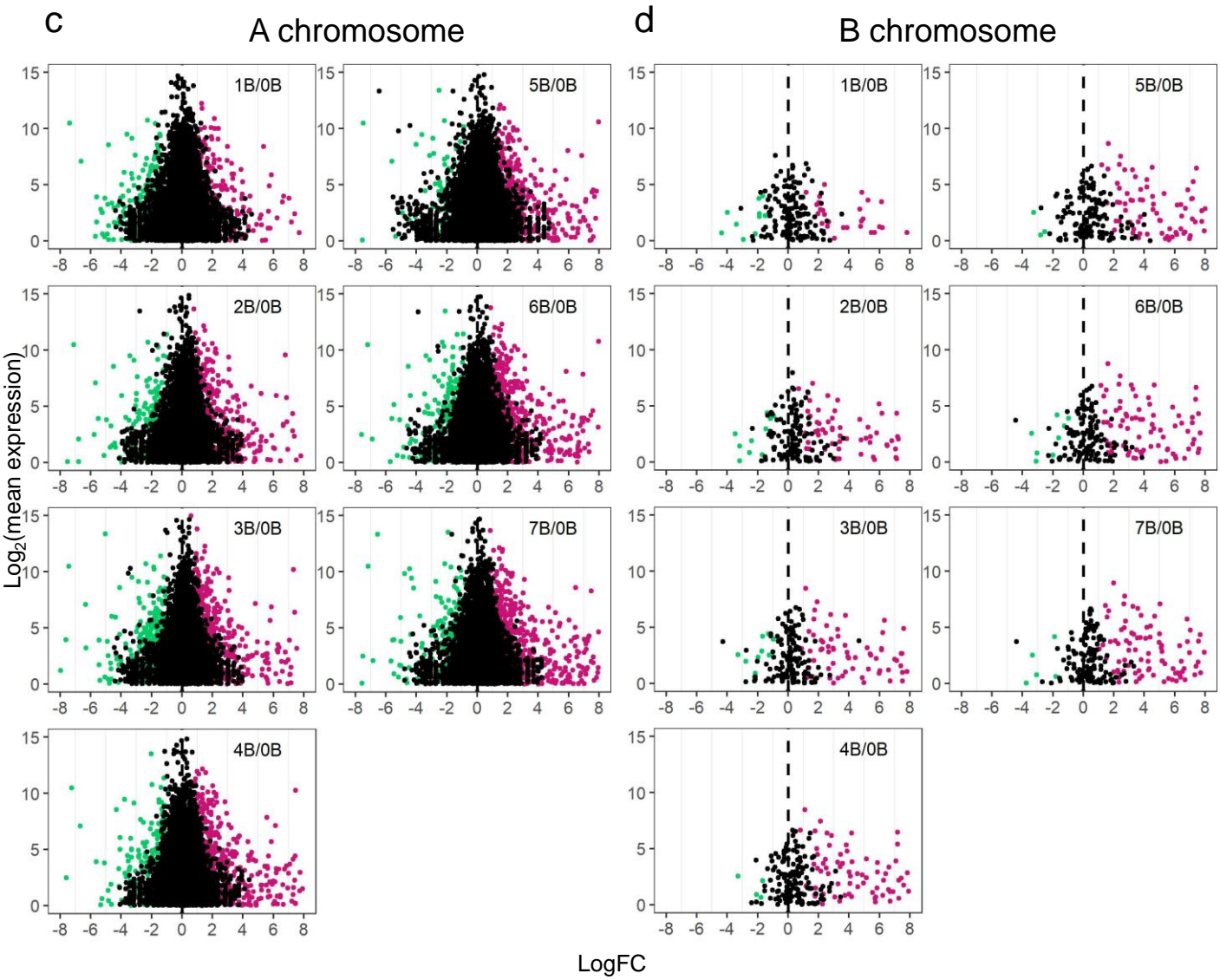


Figure S19.

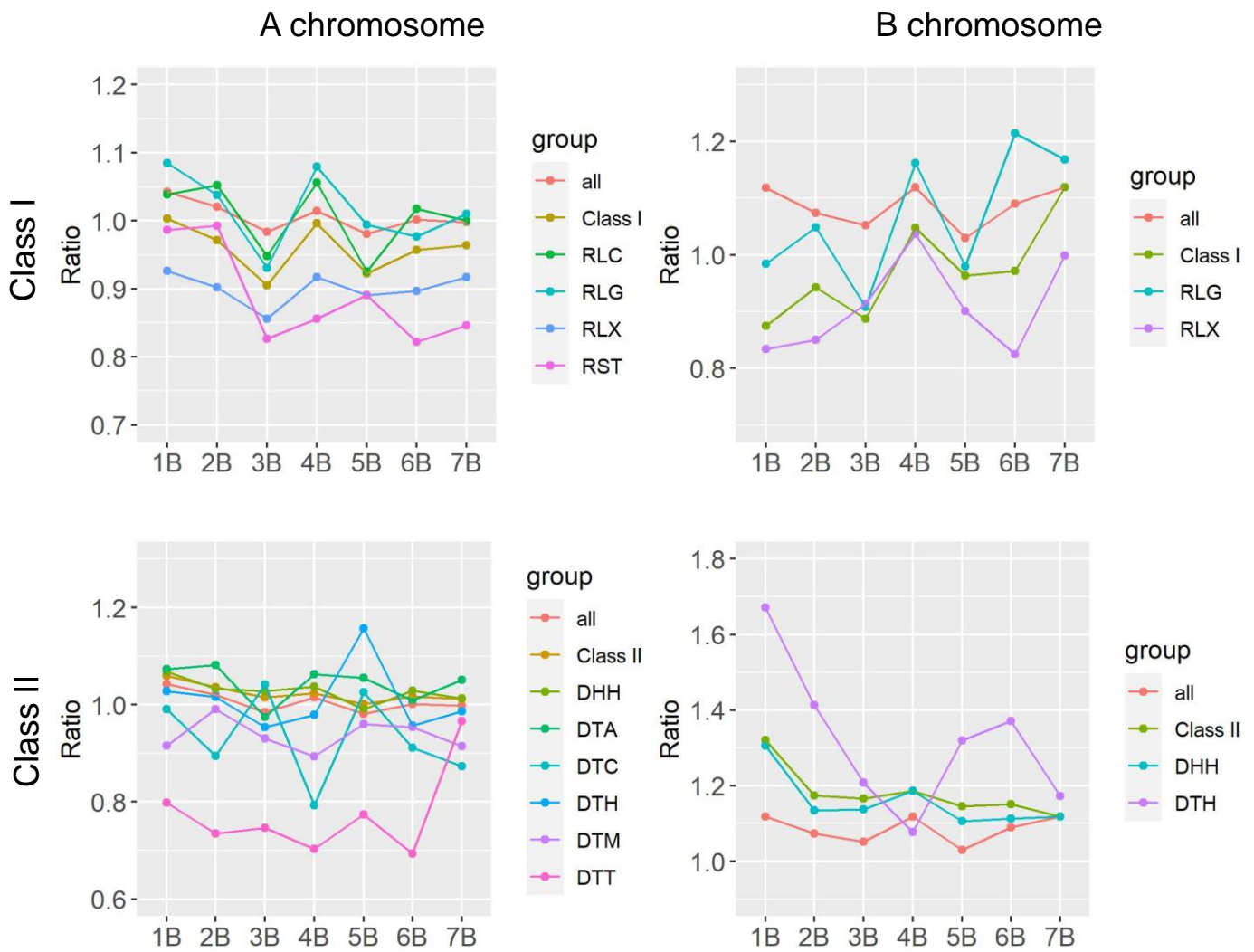
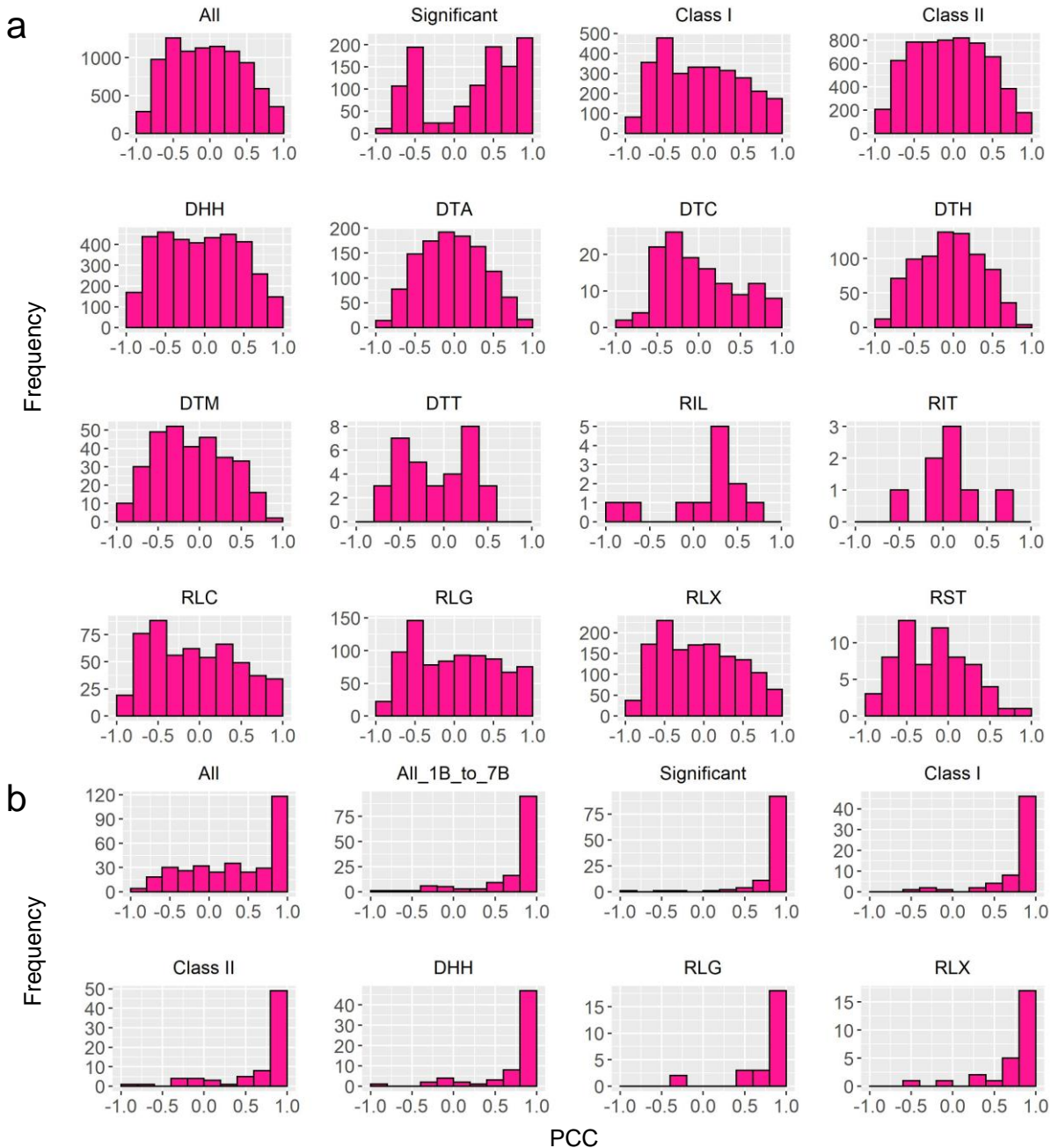


Figure S20. Median of ratios of A-located and B-located TEs in different superfamilies. The X-axis refers to the B copy number of the experimental group compared with 0B as the control group, whereas the y-axis denotes the median of ratios computed as in Table S2. Superfamilies that have over 20 elements are shown. DHH, Helitron; DTA, TIR-hAT; DTC, CACTA; DTH, TIR-PIF/Harbinger; DTM, TIR-Mu; DTT, TIR-Tc1/Mariner; DTX, class II-unclassified; RIL, LINE-L1-like; RIT, LINE; RLC, LTR-Copia; RLG, LTR-Gypsy; RLX, LTR-unclassified; RST, SINE. 'all' refers to all TEs.



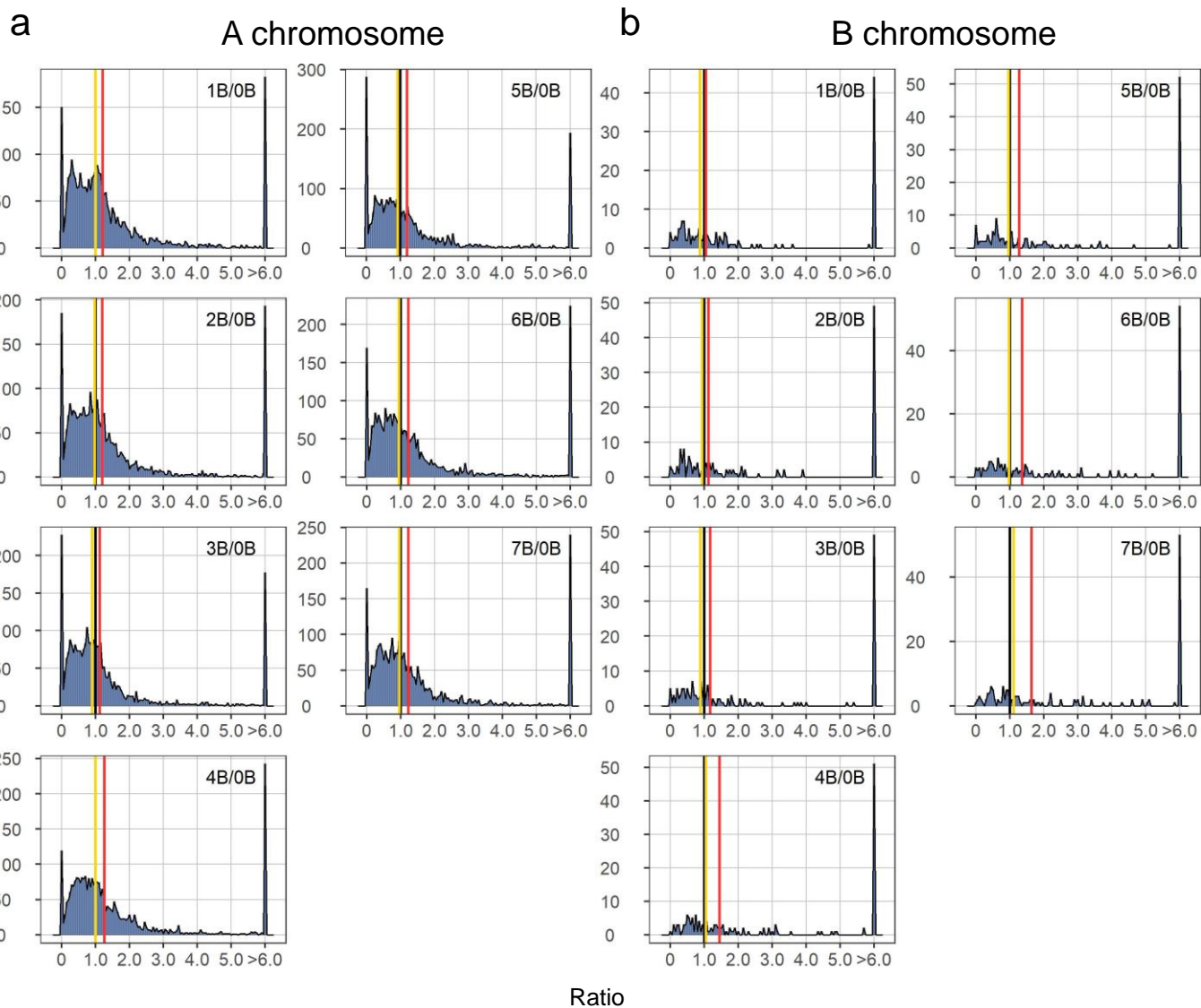


Figure S22. Ratio distributions and scatter plots of differential expression for Class I TEs. Distributions of A-located **(a)** and B-located **(b)** TEs were generated as described in Figure 1, while scatter plots of A-located **(c)** and B-located **(d)** TEs were generated as described in Figure 5.

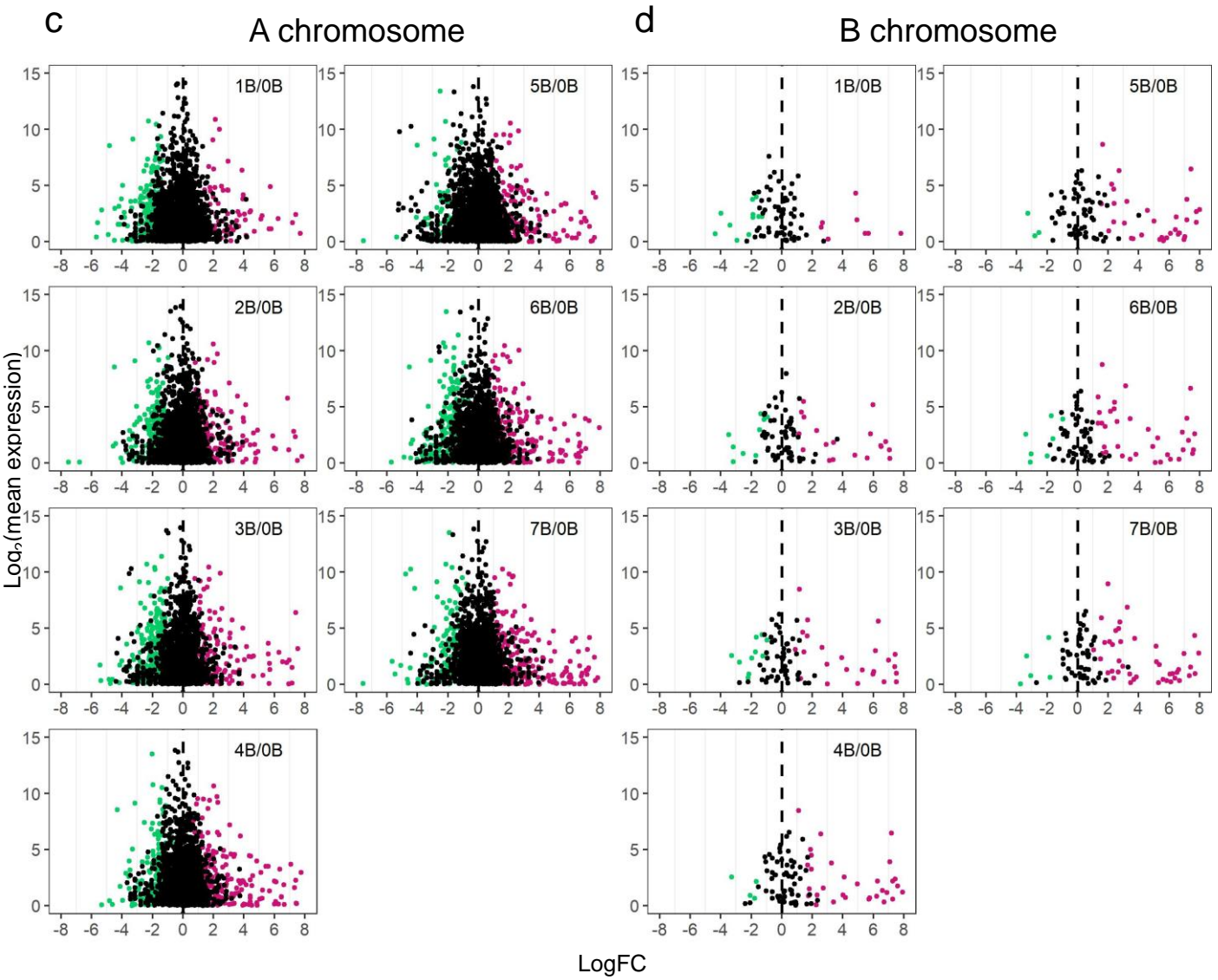


Figure S22.

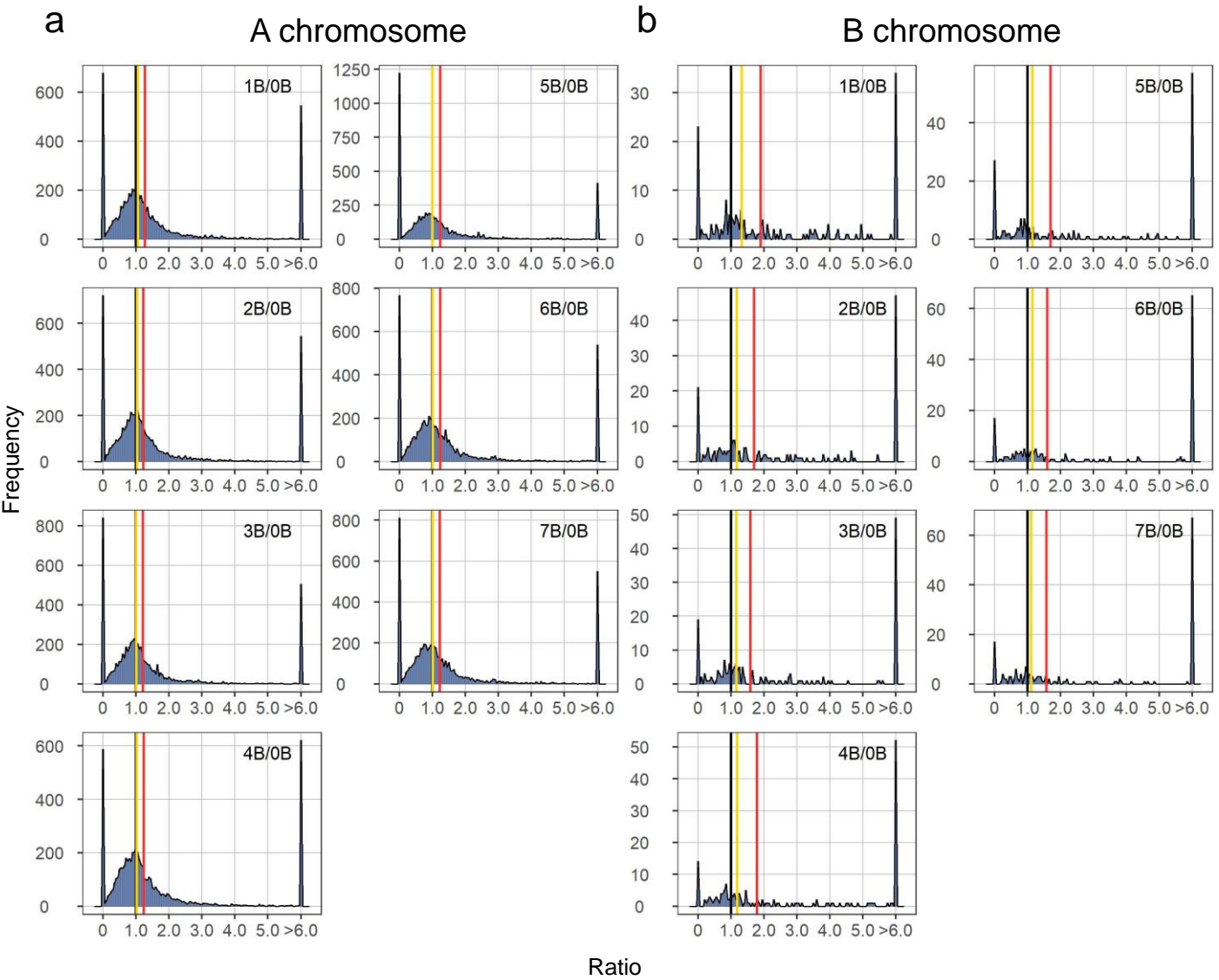


Figure S23. Ratio distributions and scatter plots of differential expression for Class II TEs. Distributions of A-located **(a)** and B-located **(b)** TEs were generated as described in Figure 1, while scatter plots of A-located **(c)** and B-located **(d)** TEs were generated as described in Figure 5.

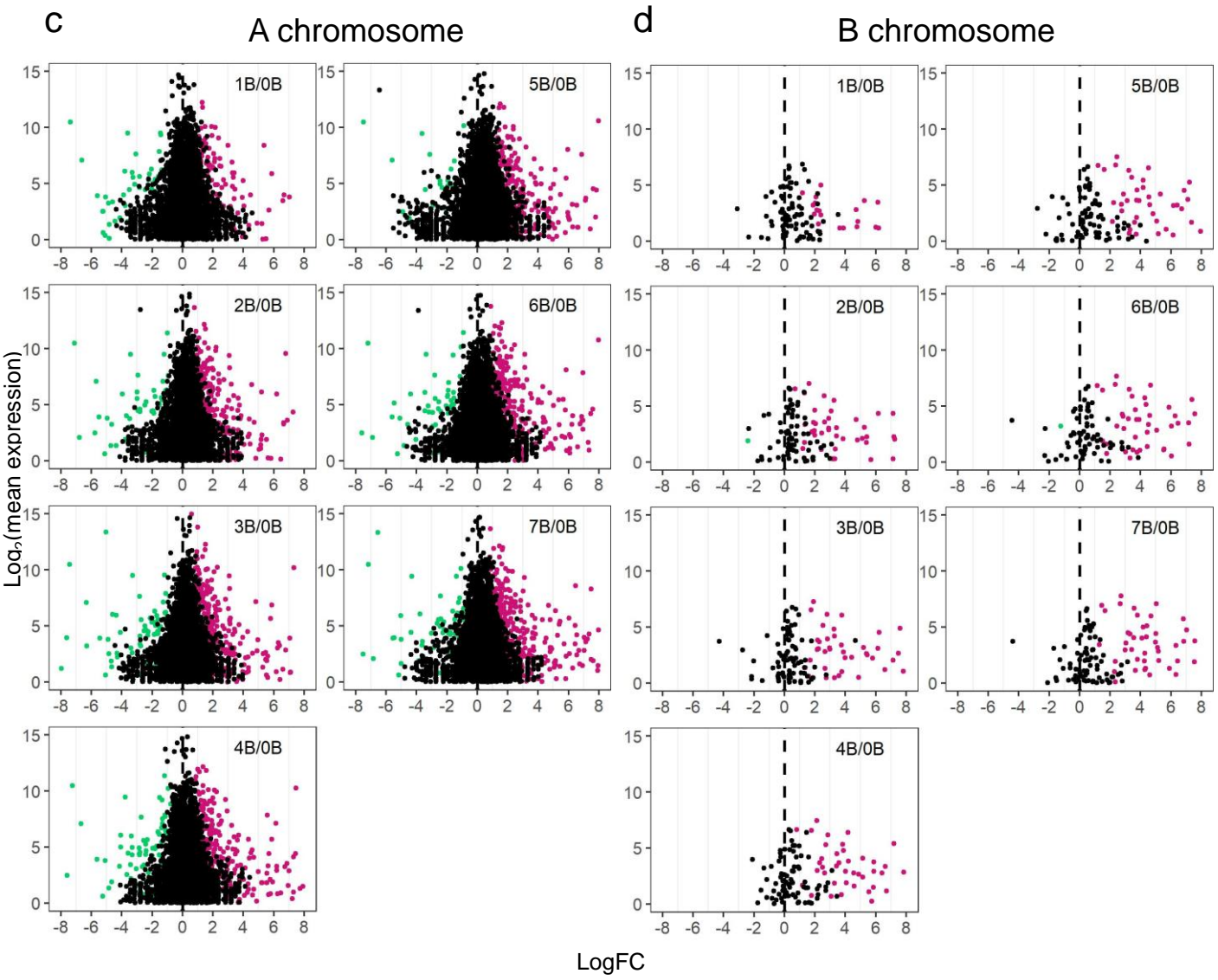


Figure S23.

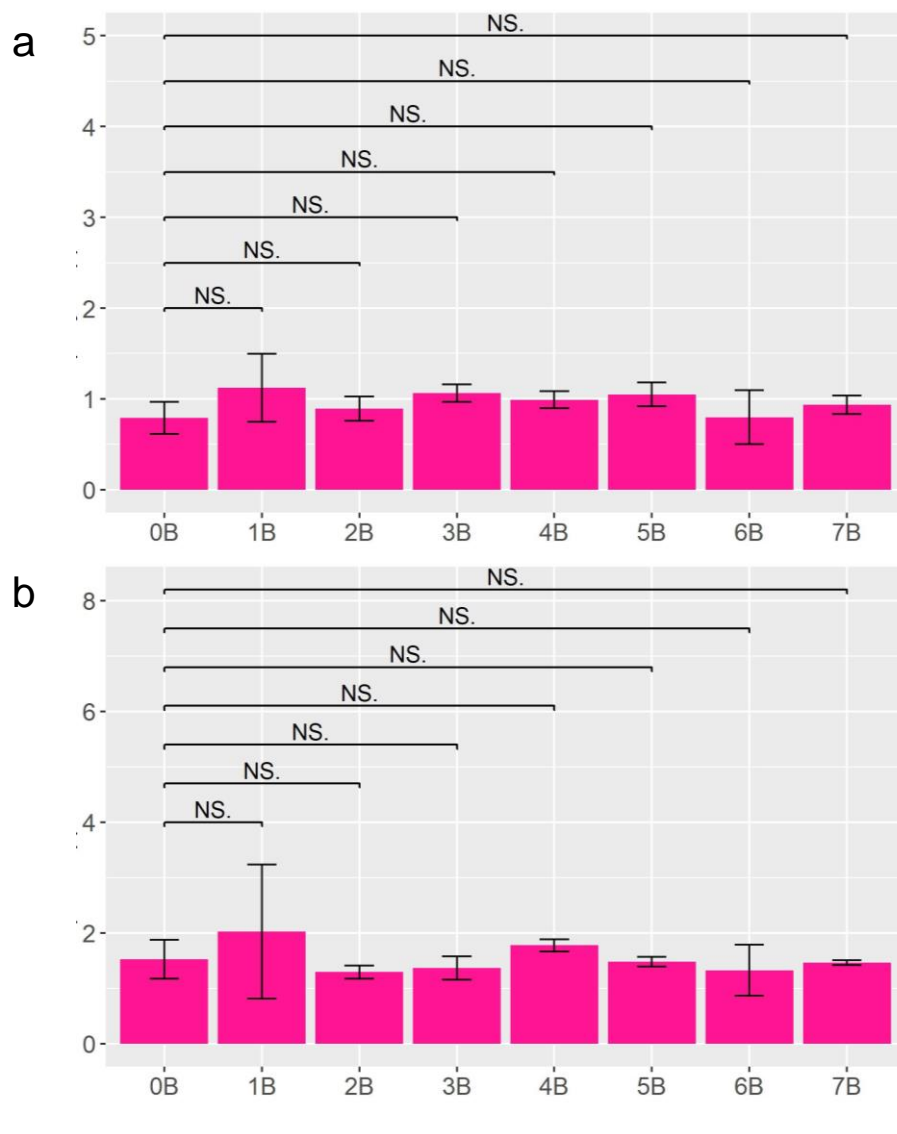


Figure S24. Ratios of reads uniquely mapped to the reference genome **(a)** and the TE exemplar **(b)** to those uniquely mapped to ERCC sequences. Read counts were averaged across biological replicates. Then ratios of averaged read counts uniquely mapped to the reference genome/ TE exemplar and those uniquely mapped to ERCC were computed and plotted on the y-axis. The x-axis denotes the genotype of plants used for RNA-seq. Error bar, SD across biological replicates. NS., Student's t-test for significance (P -value > 0.05).